The emergence of supersonic flow on wind turbines

De Tavernier, Delphine; Terzi, Dominic Von

DOI
10.1088/1742-6596/2265/4/042068

Publication date
2022

Document Version
Final published version

Published in
Journal of Physics: Conference Series

The emergence of supersonic flow on wind turbines

The emergence of supersonic flow on wind turbines

Delphine De Tavernier, Dominic von Terzi
Delft University of Technology, Kluyverweg 1, 2629HS Delft, The Netherlands
E-mail: d.a.m.detavernier@tudelft.nl

Abstract. The future generation of wind turbines will be characterised by longer and more flexible blades. These large wind turbines are facing higher Reynolds numbers, as a consequence of longer chord lengths and increased relative wind speeds. Higher tip speeds, however, also result in an increased Mach number. Although the maximum tip speed in steady design conditions may remain (well) below the critical value, the presence of turbulence, wind gusts, blade deflections, etc. in combination with the flow acceleration over the airfoil surface, may cause a significant increase in the velocity perceived over the blade surface. We have evaluated the operational conditions of the *IEA 15MW* reference turbine using OpenFAST in normal design and off-design conditions to demonstrate that, if unabated, near-future wind turbines will be at risk of suffering from local supersonic flow. The driving factor is identified to be inflow turbulence, however, the tip airfoil is also of major importance. Local supersonic flow conditions may lead to severe lifetime degradation.

1. Introduction

The wind energy industry expects significant growth in the next decades in order to meet the future energy demand, driven by the growing global population, increasing overall demand, and the need for clean, affordable and renewable energy [1]. This is according to many researchers the incentive towards even larger wind turbines with longer and more flexible blades [2]. The future generation of such giant wind turbines will bring new aerodynamic challenges.

Large wind turbines are facing higher (chord-based) Reynolds numbers (RE) exceeding 10×10^6 as a consequence of longer chord lengths and increased relative wind speeds. Various researchers have evaluated the effect of the Reynolds number on the aerodynamic behaviour of airfoils and its influence on the turbine performance, turbine operation and the design of a wind turbine rotor. Within the EU FP7 AVATAR project (AdVanced Aerodynamic Tools of lArge Rotors), high Reynolds number (but low Mach number) wind tunnel tests on 2D airfoil sections have been performed with the aim to gather reliable validation data within a representative operational range. The experimental campaigns were performed at the LM Wind Power in-house wind tunnel for chord-based Reynolds numbers up to 6×10^6 and at the DNW High Pressure Wind Tunnel in Göttingen (HDG) for chord-based Reynolds numbers up to 15×10^6 on the DU00-W-212 airfoil [3, 4]. At Princeton University, a compressed-air wind tunnel is used to experimentally investigate the aerodynamic performance of 2D airfoil sections [5], but also the power and thrust coefficient of a horizontal-axis wind turbine as a function of the Reynolds number [6]. Later, they also characterized the wake behind a horizontal-axis wind turbine at high Reynolds numbers representative for full-scale wind turbines [7].

Higher tip speeds also result in an increased Mach number. Sørenson et al. [8] state that for large wind turbines with a rotor radius in the order of 100 m, the blade tip might reach

high relative velocities approaching thirty percent of the speed of sound, suggesting that the incompressible assumption might be violated in the tip region of the turbine. In their study, they investigated, through computational fluid dynamics, the effects of compressibility on 2D airfoil aerodynamics and the possibility of correcting incompressible flow solutions using explicit compressibility corrections. Other researchers such as Yan [9] or within the AVATAR project [10] assessed compressibility effects on the performance of (large) horizontal-axis wind turbines.

While most wind turbine studies focus on subsonic flows, transonic or supersonic flows remain mostly ignored in the wind turbine literature. Two studies have been found in which wind turbines are linked to high speed flow conditions. Wood [11] studied how the action of shock-stall, and thus significantly increased drag, may provide an inherent mechanism for over-speed protection for small wind turbines operating at a high tip speed ratio. Hossain et al. [12], on the other hand, studied the propagation of shocks on the NREL Phase VI wind turbine airfoil at a Mach number of 0.8, but it is Sørenson's [8] opinion that transonic conditions are not especially relevant for the envisioned normal operation of large scale wind turbines.

Although the maximum tip speed in steady design conditions may remain (well) below supersonic conditions, the presence of turbulence, wind gusts, or blade/turbine deflections may cause a significant increase in the velocity perceived by the blades. Additionally, the flow over the airfoil surface is accelerated up to four times the inflow velocity, depending on the suction peak in the airfoil pressure distribution. This may eventually lead to transonic conditions, and thus flow velocities locally reaching the supersonic regime, even at relatively low inflow velocities. The appearance of local supersonic flow on the airfoil would likely cause shock induced flow separation and bears the distinct risk of buffeting or stall. If not mitigated, this could result in a severe lifetime degradation through the concomitant vibrations.

Therefore, we hypothesize that "if unabated, future wind turbines, characterized by long and slender blades, will be at risk of suffering from supersonic flow." It is the objective of this study to evaluate (1) what operational conditions are required to locally reach supersonic flow, (2) whether and how often these operational conditions may occur on (near-)future wind turbines, within the design space, but also in off-design conditions and (3) how sensitive these conditions are to environmental and turbine-specific parameters such as airfoil design, floating motion or turbulence, for example.

2. Methodology

2.1. Supersonic flow over an airfoil

The pressure distribution along the airfoil contours dictates a velocity profile. At the point of minimum pressure coefficient, the maximum flow velocity is expected. The pressure distribution, and the associated pressure peak, at a fixed Reynold number and angle of attack can be determined using an integral boundary-layer method, such as employed by Xfoil [13].

The pressure peak is compared to the critical pressure coefficient. Equation 1 prescribes a relation to determine the critical pressure coefficient $C_{p,crit}$ at which the flow over the airfoil is locally just attaining the critical Mach number M_{crit}. The atmosphere is defined by the specific heat ratio γ and the Mach number of the freestream inflow M_∞. In Figure 1a, this relation is visualized for a critical Mach number equal to $M_{crit} = 1$, $M_{crit} = 0.9$ and $M_{crit} = 0.8$.

$$C_{p,crit} = \frac{2}{\gamma M_\infty^2} \cdot \left(\left[\frac{1 + \frac{1}{2}(\gamma - 1) M_\infty^2}{1 + \frac{1}{2}(\gamma - 1) M_{crit}^2} \right]^{\frac{\gamma}{\gamma - 1}} - 1 \right) \tag{1}$$

The critical pressure coefficient, as given by Equation 1, corresponds to compressible flow conditions. By applying the Prandtl-Glauert compressibility correction, given by Equation 2, the critical compressible pressure coefficient ($C_{p,c}$) is converted to an incompressible ($C_{p,i}$)

equivalent. The Prandtl-Glauert correction depends on the inflow Mach number, defined here with a constant speed of sound $c = 340.3m/s$ according to ISA at sea level.

$$C_{p,c} = \frac{C_{p,i}}{\sqrt{1 - M_\infty^2}}, \text{ where: } M_\infty = \frac{V_\infty}{c} \tag{2}$$

From the airfoil pressure peak and the definition of the critical pressure coefficient (Figure 1a), the critical combination of the angle of attack and inflow velocity is identified for which locally the critical pressure coefficient is attained. The boundary of the supersonic regime, as shown in Figure 1b for $M_{crit} = 1$, depends significantly on the airfoil shape but is also affected by e.g. the Reynolds number or early transition.

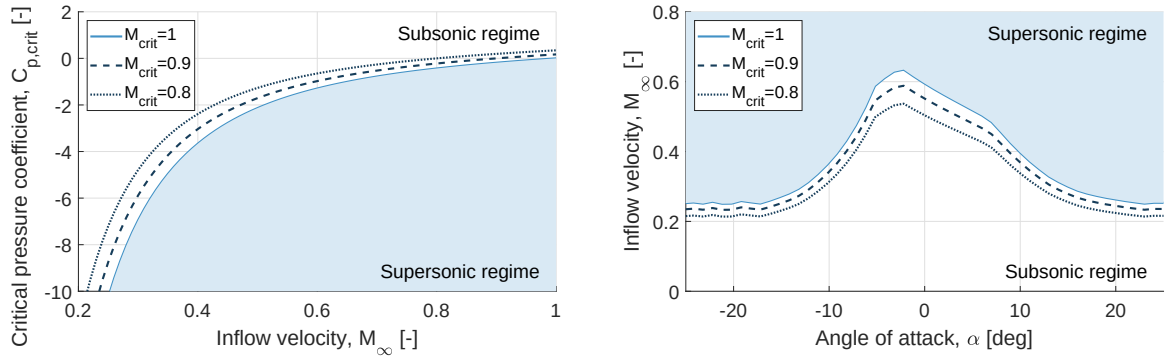

(a) *(b)*

Figure 1. (a) Critical pressure coefficient as a function of inflow velocity for a critical Mach number of 1, 0.9 and 0.8. (b) The critical combination of the angle of attack and inflow velocity for which locally the critical Mach number is reached. The boundary is derived for the FFAW3211 airfoil at $RE = 15 \times 10^6$.

2.2. Turbine design and simulation tool

To identify whether a near-future turbine will experience local supersonic flow conditions, the floating variant of the *IEA 15MW* turbine is considered as reference. This floating turbine configuration is selected as it mirrors the wind industry's trend of offshore machines. The *IEA 15MW* turbine [14] has a rotor radius of $120m$, a maximum tip speed of $95m/s$ and operates in a wind regime from 3 to $25m/s$. The turbine is set on a semi-submersible floating platform with a chain catenary mooring system. The so-called *Umaine VolturnUS-S* [15] floating platform is a four-column construction with the turbine located at the center of the platform. The floating variant of the *IEA 15MW* turbine has a floating-specific tower and a modified floating-specific controller.

The turbine's operational conditions are evaluated using the open-source software OpenFAST [16]. OpenFAST enables coupled nonlinear aero-hydro-servo-elastic simulation in the time domain. It allows multi-physics, multi-fidelity simulations of the coupled dynamic response of wind turbines. The OpenFAST model inputs are extended from the repository developed within the IEA Wind Task 37 [17]. TurbSim [18] is used to generate a stochastic, turbulent wind field with various mean wind speeds. For each simulation, six seeds with an independent wind field are set-up. Each seed covers a timespan of 10 minutes. The first few seconds are disregarded to avoid the transient behaviour in the analysis. The simulation time step is set to $0.025s$. The operational conditions, with an emphasis on the relative inflow velocity and angle of attack, are tracked in time at various discrete spanwise locations.

The operational conditions are monitored in a range of events, mapping both cases within the design space and in off-design conditions. For the normal design condition, indicated as the baseline case, a normal turbulence wind profile, representative for class A, with a shear coefficient of $k = 0.2$ is generated. The sea state is prescribed by regular waves, identified by the significant wave height and peak period. These parameters are depending on the reference wind speed and are defined according to the IEA design standards (IEC 61400-1 [2020], summarized in [15]). Variations to the baseline case are made in order to represent various off-design conditions. Here, deviations are made in terms of inflow turbulence, floating motion, aero-elastic behaviour, pitch offset and the tip airfoil. These off-design conditions will serve as the basis of a sensitivity study.

3. Results

3.1. Normal design conditions

The reference *IEA 15MW* turbine is simulated in normal design conditions for a site of class A. As a standard, the floating motion and aero-elastic deflection of the blades and the tower are enabled.

In Figure 2 the turbine response, in terms of angle of attack (Figure 2b) and relative velocity (Figure 2c) at the blade tip, is visualised for a mean inflow velocity slightly below the rated wind speed ($V_{ref} = 10m/s$). The turbulent wind profile at hub height is presented in Figure 2a.

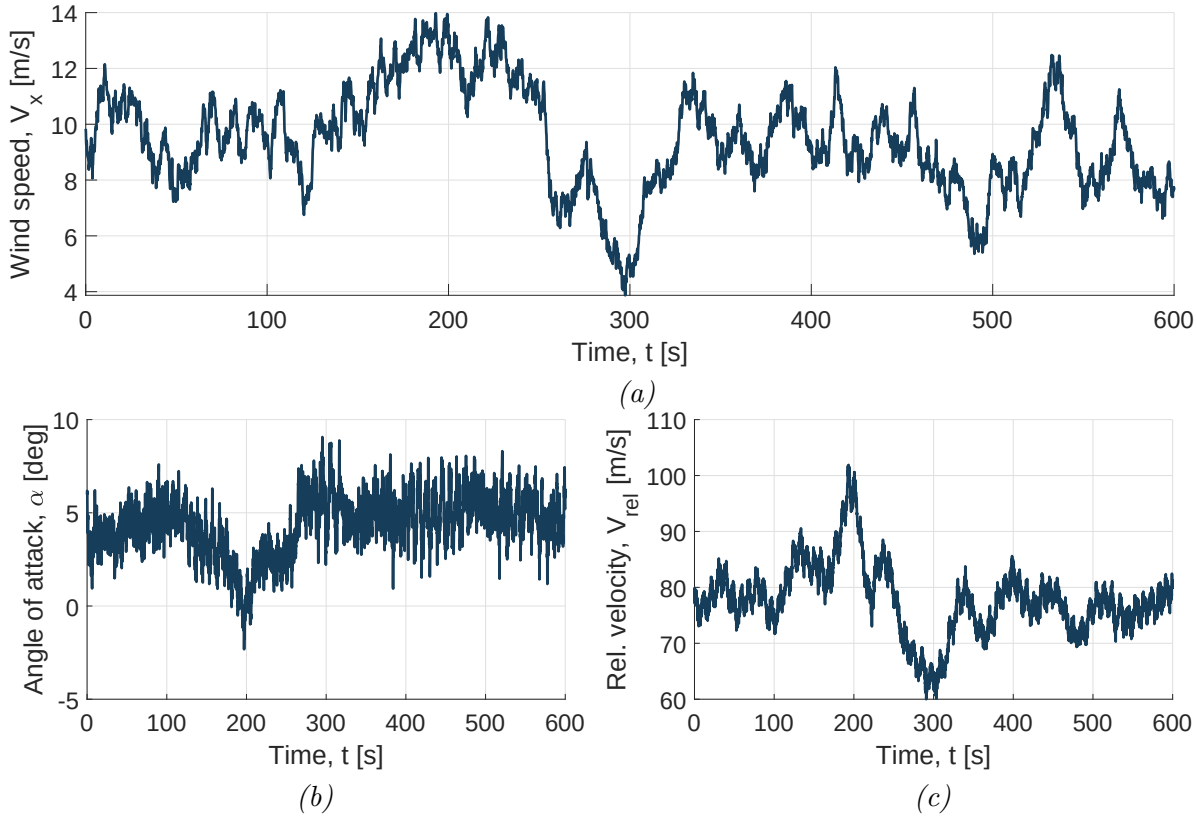

Figure 2. (a) Turbulent inflow of class A with a reference wind speed of $10m/s$. (b) Corresponding angle of attack variation at $r/R = 0.97$. (c) Corresponding relative velocity experienced by the blade at $r/R = 0.97$.

Combining this information allows to generate Figure 3a, where the angle of attack is plotted

versus the relative velocity experienced by the blade tip. Here, every dot represents one distinct time step. The blue area indicates the supersonic regime, as explained before. Around the rated wind speed, the wind turbine is operating at its maximum rotational speed and optimal pitch angle. Considering Figure 3a, one may observe that the local flow conditions over the tip airfoil remain well below the supersonic regime.

However, as the wind speed increases, the blades pitch out in order to keep the power output constant, while the rotational speed remains at its maximum. Near cut-out, the blades are pitched out more than 20 degrees and this causes the angle of attack to reduce significantly. The relative velocity increases slightly due to the increased wind vector component. Figure 3d reveals that at this high wind condition, the data cloud has shifted towards the left and the blade tips are experiencing transonic conditions.

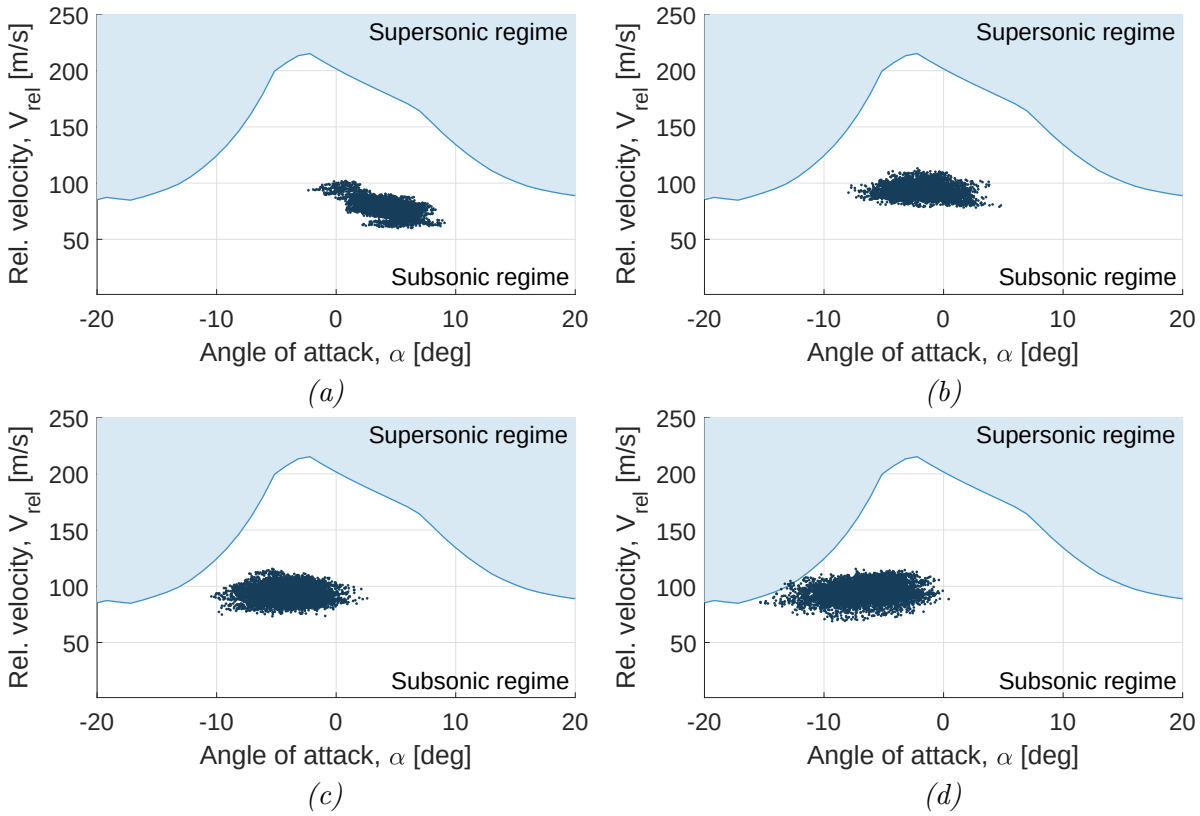

Figure 3. Operational conditions of IEA15 MW turbine at $r/R = 0.97$ in normal turbulent wind of class A at (a) 10m/s, (b) 15m/s, (c) 20m/s and (d) 25m/s. The supersonic boundary is derived for the tip-airfoil FFAW3211 at $RE = 10 \times 10^6$.

This information may be summarized for all wind speeds using a box-plot chart, shown in Figure 4a. The main line indicates the median value of the locally achieved Mach number (at the blade tip). The thin vertical lines indicate the minimum and maximum Mach number seen by the blade while the bars show the 25-75 percentile (or 50 percent of the data) and the 10-90 percentile (or 80 percent of the data). The width of the percentiles essentially expresses how the data is spread.

At low wind speeds, the operational conditions of the *IEA 15MW* turbine remain well below the supersonic boundary. It is only when the wind speed exceeds $20m/s$ that the conditions approach local Mach numbers near 1. While Figure 4a focusses only on the tip region of the blade, Figure 4b zooms in on the higher wind speeds but for various spanwise locations going from

$r/R = 0.8$ to $r/R = 0.97$. As expected, the local Mach number decreases when approaching the root, mostly because of the smaller rotational velocity component. However, in normal operation, it is the outboard 7.5% of the blade that is at risk to experience supersonic flow over the blades. In the following discussions, we will focus only on the spanwise location $r/R = 0.97$ except stated otherwise.

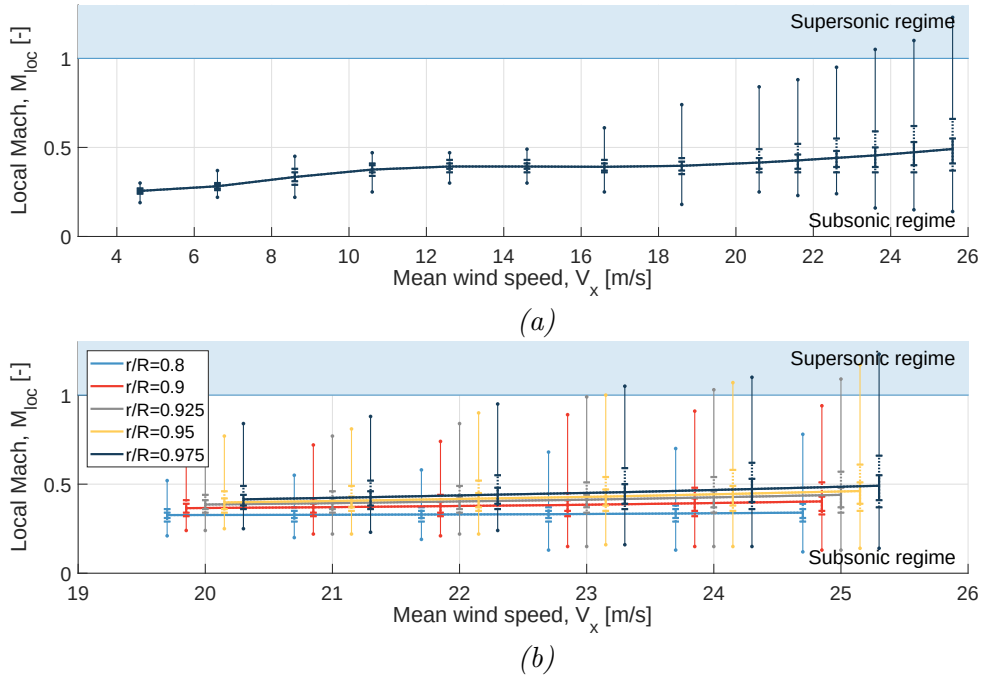

Figure 4. Locally achieved Mach number for different mean inflow conditions (a) at $r/R = 0.97$ and (b) at various spanwise locations. The supersonic boundary is derived for the tip-airfoil FFAW3211 at $RE = 10 \times 10^6$; ▯ 25-75 percentile, ⋮ 10-90 percentile and | the min/max.

3.2. Off-design conditions

To understand what is driving the turbine into local supersonic conditions, a sensitivity study is performed. The operational conditions are re-evaluated in slightly deviating design or operating settings. Five categories are considered: floating motion, aero-elastic behaviour, inflow turbulence, pitch offset and the tip airfoil. The different levels per category are summarized in Table 1. The obvious sensitivity to the turbine rotational speed is disregarded in this study. The sensitivity study is only presented here for wind speeds between 20 and 25m/s and at an outboard section at $r/R = 0.97$. The results combine the simulations of all six wind inflow seeds performed per simulation. The inflow seeds, if applicable, are kept identical in the sensitivity study for a fair comparison.

Table 1. Summary of the cases considered in the sensitivity study. The baseline case is indicated in bold.

Category	Level 1	Level 2	Level 3	Level 4
1 - Floating motion	Bottom-fixed	**Normal waves**	Large waves	
2 - Aero-elasticity	Rigid	**Flexible**		
3 - Inflow turbulence	NTM-C	NTM-B	**NTM-A**	ETM-A
4 - Pitch offset	+2 deg	**0 deg**	-2 deg	
5 - Tip airfoil	NACA64618	**FFAW3211**	DU93W210	

1 - Floating motion: The first parameter is the floating motion. Three cases are considered: no floating motion, floating motion caused by normal waves and floating motion due to large waves, both defined according to IEC standard load cases (DLC1.1 and DLC1.6 of IEC 61400-1 [2020], summarized in [15]). Floating turbines are experiencing translations and rotations in six degrees of freedom, affecting the local angle of attack and relative velocity perceived by the blades. Although larger angle of attack variations may be expected for floating turbines, Figure 5a shows that the local Mach number at the blade tip is not affected significantly. As such the floating motion is not identified as a driving factor pushing turbines towards supersonic flow conditions. However, it is noteworthy to state that one could expect that floating offshore turbines will be at larger risk. This is supported by the fact that offshore sites usually have higher wind resources and that turbines generally tend to have a higher tip speed since noise is less of an issue. Additionally, it should be mentioned that the additional turbulent effects due to blade-wake interaction resulting from the floating motion is not incorporated in the performed OpenFAST calculations.

Aero-elasticity: To identify the effect of the aero-elastic behaviour, a comparison is made between a turbine with a rigid and flexible tower and blades. Here, a similar conclusion as for the floating motion can be made. While the aero-elastic deflections may introduce larger angle of attack and relative velocity variations, the effect on the local Mach number distribution is fairly limited. The mean value and percentile domains are very similar. In fact, in terms of the maximum achieved Mach number, flexible blades are slightly in the advantage. This is shown in Figure 5b. Also here, the additional effects due to blade-wake interaction resulting from the aero-elastic deflection is not included in the calculations.

Inflow turbulence: To elucidate the importance of inflow turbulence, a study is performed on the floating *IEA 15MW* turbine operating in a normal turbulent inflow corresponding to class A, B and C, as well as extreme turbulence of class A. Figure 5c summarizes the locally achieved Mach numbers at the blade tip ($r/R = 0.97$). While the mean value is rather constant for all four cases, the maximum achieved Mach number significantly increases with turbulence intensity. In highly turbulent inflow, more data points are entering the supersonic regime. For the most extreme turbulent case (ETM-A), the maximum achieved Mach number exceeds $M = 1.4$, while $M = 1$ exists already from a mean inflow velocity of $20m/s$. From this, it may be concluded that the inflow turbulence is one of the driving factors for supersonic flow conditions on wind turbines. In fact, this follows the expectations since in steady conditions, the turbine's operational conditions remain well below the supersonic regime.

Pitch offset: The actual blade angle of attack may deviate from what is calculated with OpenFAST. This may be caused by the lack of including physical phenomena in the simulations such as blade torsion caused by bend-twist coupling or blade-wake interaction originating from aero-elastic behaviour or the floating motion. It may also result from abnormal operation of the turbine by for example a malfunctioning of the controller, yaw off-set, etc. To identify the effect of a small distortion in the blade angle of attack, a pitch offset of plus and minus 2 deg is introduced to one of the blades. The results are summarised in Figure 5d. Here, not only the maximum attained Mach number is affected but also the mean value and data distribution. With a -2deg pitch off-set, the turbine's operational conditions are pushed towards the supersonic regime. For a $+2$deg off-set, the opposite is true. This study identifies how sensitive the results are to an accurate prediction of the angle of attack.

Tip airfoil: The final sensitivity, evaluated in this study, is the airfoil at the tip. As explained in subsection 2.1, the flow acceleration over the airfoil surface depends on the pressure peak. The size of this pressure peak at a given angle of attack is significantly affected by the airfoil choice. To highlight the role of the airfoil selection, three different wind energy airfoils are compared: FFAW3211 (i.e. the tip airfoil of the *IEA 15MW*), NACA64618 and DU93W210. For this evaluation, only the supersonic boundary curve is updated and thus the turbine design

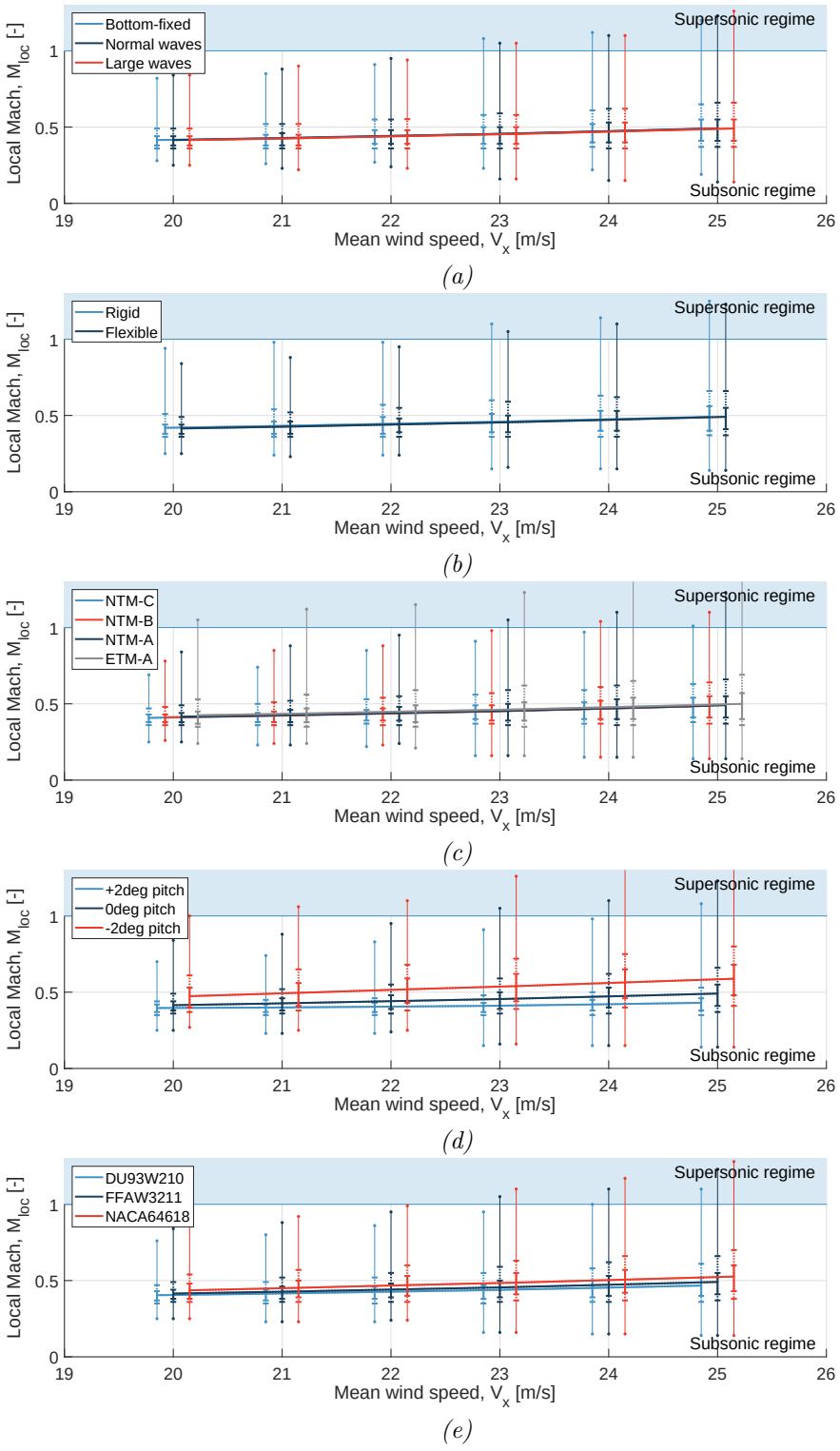

Figure 5. Locally achieved Mach number at $r/R = 0.97$ for various off-design conditions. Sensitivity study on five categories: (a) floating motion, (b) aero-elasticity, (c) inflow turbulence, (d) pitch offset and (e) tip airfoil. The supersonic boundary is derived for tip-airfoil FFAW3211 at $RE = 10 \times 10^6$; ⌶ 25-75 percentile, ⌶ 10-90 percentile and | the min/max.

remains untouched. The results are provided in Figure 5e. The tip airfoil can significantly affect the distribution of the locally achieved Mach number. The NACA64618 shows a larger suction peak close to the airfoil leading edge at high angles compared to the other two airfoils and thus higher local Mach numbers are achieved here. As such, if properly chosen, tip airfoil with limited pressure peaks could keep the turbine out of the supersonic regime. Finally, note that lower Reynolds numbers or early transition generally reduce the suction peak. This is mostly visible at higher angles of attack, but its effect remains marginal.

4. Discussion

The previous analysis proved that in various conditions, both within the design space and in off-design conditions, the *IEA 15MW* turbine may experience supersonic flow over the blade's surface. However, a remaining question is how often local supersonic flow occurs on the turbine and what its effect is on the turbine itself. For this, an analysis is performed on identifying the occurrence.

Occurrence can be understood in various ways. Firstly, it may be approached as in how many seeds supersonic flow appears. Three sets of simulations are compared: the baseline case, extreme turbulence and extreme turbulence with a negative pitch off-set of 2 deg. Figure 6a shows that in the more extreme situation, already from $21m/s$ supersonic flow appears at least once in every seed. For the baseline case, it is in 80% of the seeds that supersonic flow appears at $25m/s$.

A second approach towards identifying the occurrence is: if supersonic flow appears in a 10 minute interval, for how many seconds does it occur. This is presented in Figure 6b for the same three sets of simulations. For the baseline case, the turbine experiences supersonic flow conditions in the order of one second per 10 minute interval. In the more extreme situations, this could go up to 15 seconds in a 10 minute interval. While this intuitively may feel fairly limited, in the entire turbine's lifetime this adds up rather quickly.

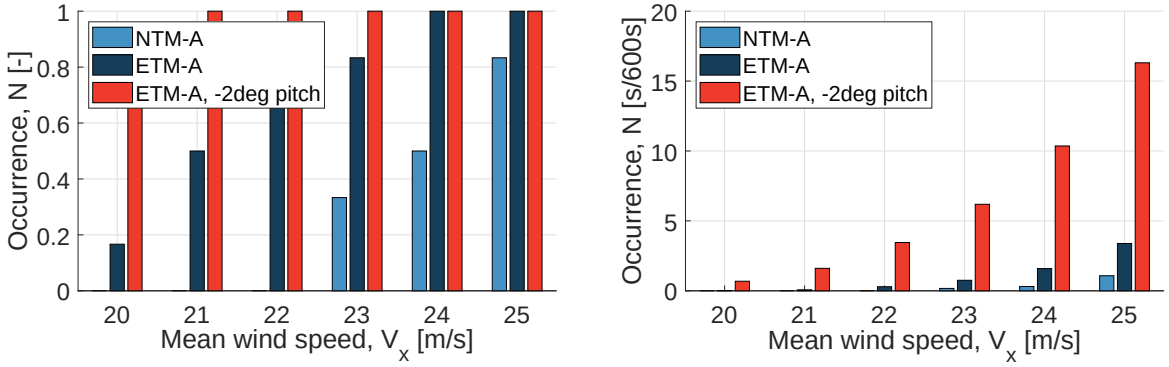

(a) *(b)*

Figure 6. The occurrence of supersonic in terms of (a) seeds and (b) seconds per 10 minute interval.

The amount of research performed on wind turbine airfoils in transonic/supersonic conditions is very limited. Therefore, it is still unclear how the flow will react when (shortly) entering into these flow conditions. One could expect that locally exceeding $M = 1$ can cause separation of the boundary layer at the point where transonic flow is reached. This can lead to full separation and stall of the profile, higher drag and even shock buffeting. Dynamic effects may also play a significant role in the behaviour of the flow over the blades. On turbine level, the consequences

of supersonic flow may concern noise issues, performance loss or turbine lifetime degradation, but more research is required to be able to quantify this further.

Finally, a note should be made on the limitations of this study. When characterising the airfoils and the turbine operational conditions, we are relying on incompressible tools with some compressibility corrections. While these tools might no longer be very credible in these remarkable operational ranges, it is believed that the main message of this study, that supersonic flow conditions may appear on near-future wind turbines, still holds.

5. Conclusions

This paper demonstrates the possibility of supersonic flow on near-future wind turbines. The simulation tool OpenFAST is used to identify the operational conditions, in terms of angle of attack and relative velocity along the blade span, of the *IEA 15MW* reference turbine within the design space and in off-design conditions.

We identified that for the *IEA 15MW* reference turbine supersonic flow may appear at the blade tip and at high wind speeds. In normal operational conditions, local Mach numbers above one appeared near the cut-out wind speed, while in off-design conditions supersonic flow appears at lower wind speeds as well. The inflow turbulence is identified as the driving factor. Small deviations to the angle of attack and the airfoil selection at the tip may drive the turbine towards or away from the supersonic regime. Supersonic flow is not occurring constantly but for a limited amount of time. The exact consequence on the flow and turbine still needs to be evaluated in future research.

Following the design and market trends, it is likely that supersonic conditions will become more likely for future turbines if not accounted for in the design or operational strategy. This study proves that the assumption of low Mach numbers should be reconsidered. Supersonic flow for wind turbines will pose a set of new research questions in which the impact of supersonic physics such as compressibility, shock waves, buffeting, etc. on wind turbine performance and lifetime needs to be evaluated and mitigated.

References

[1] Veers P, Dykes K, Lantz E, Barth S, Bottasso C L, Carlson O, Clifton A, Green J, Green P, Holttinen H, Laird D, Lehtomäki V, Lundquist J K, Manwell J, Marquis M, Meneveau C, Moriarty P, Munduate X, Muskulus M, Naughton J, Pao L, Paquette J, Peinke J, Robertson A, Rodrigo J S, Sempreviva A M, Smith J C, Tuohy A and Wiser R Grand challenges in the science of wind energy 2019 *Science* **366**

[2] von Terzi D and Bottasso C L Mini-symposium: wind turbine and plant optimization beyond LCoE 2021 *Proceedings of WESC21 conference*

[3] Pires O, Munduate X, Ceyhan O, Jacobs M and Snel H Analysis of high Reynolds numbers effects on a wind turbine airfoil using 2D wind tunnel test data 2016 *Journal of Physics: Conf. Series* **753** 022047

[4] Pires O, Munduate X, Ceyhan O, Jacobs M, Madsen J and Schepers J G Analysis of the high Reynolds number 2D tests on a wind turbine airfoil performed at two different wind tunnels 2016 *Journal of Physics: Conf. Series* **749** 012014

[5] Brunner C E, Kiefer J, Hansen M O L and Hultmark M Study of Reynolds number effects on the aerodynamics of a moderately thick airfoil using a high-pressure wind tunnel 2021 *Experiments in Fluids* **62**

[6] Miller M A, Kiefer J, Westergaard C, Hansen M O L and Hultmark M Horizontal axis wind turbine testing at high Reynolds numbers 2019 *Physical Review Fluids* **4**

[7] Piqué A, Miller M A and Hultmark M Characterization of the wake behind a horizontal-axis wind turbine (hawt) at very high Reynolds numbers 2020 *Journal of Physics: Conf. Series* **1618** 062039

[8] Sørenson N N, Bertagnolio F, Jost E and Lutz T Aerodynamic effects of compressibility for wind turbines at high tip speeds 2018 *Journal of Physics: Conf. Series* **1037** 022003

[9] Yan C and Archer C L Assessing compressibility effects on the performance of large horizontal-axis wind turbines 2018 *Applied Energy* **212** 33–45

[10] Sørensen N N, Gonzalez-Salcedo A, Martin R, Jost E, Pirrung G, Rahimi H, Schepers G, Sieros G, Madsen H A, Boorsma K, Garcia N R, Voutsinas S and Lutz T 2017 Engineering models for complex inflow situations Report 2.8 AVATAR project

[11] Wood D H Some effect of compressibility on small horizontal-axis wind turbines 1997 *Renewable Energy* **10** 11–17
[12] Hossain M A, Huque Z and Kammalapati R R Propagation of shock on NREL phase VI wind turbine airfoil under compressible flow 2013 *Journal of Renewable Energy* **2013** 653103
[13] Drela M 1989 *Xfoil: an analysis and design system for low Reynolds number airfoils* Low Reynolds number aerodynamics (United States of America: Springer-Verlag)
[14] Gaertner E, Rinker J, Sethuraman L, Zahle F, Anderson B, Barter G, Abbas N, Meng F, Bortolotti P, Skrzypinski W, Scott G, Feil R, Bredmose H, Dykes K, Shields M, Allen C and Viselli A 2020 Definition of the IEA wind 15-megawatt offshore reference wind turbine Report NREL/TP-5000-75698 National Renewable Energy Laboratory
[15] Allen C, Viselli A, Dagher H, Goupe A, Gaertner E, Abbas N, Hall M and Barter G 2020 Definition of the UMaine VolturnUS-S reference platform developed for the IEA wind 15megawatt offshore reference wind turbine Report NREL/TP-5000-76773 National Renewable Energy Laboratory
[16] National Renewable Energy Laboratory Openfast v2.4.0 `https://github.com/openfast/openfast/` online; Accessed on 29-07-2021
[17] IEA Wind Task 37 Model data for the 15 MW offshore reference turbine `https://github.com/IEAWindTask37/IEA-15-240-RWT` online; Accessed on 06-01-2022
[18] National Renewable Energy Laboratory Turbsim v1.5.0 `https://www.nrel.gov/wind/nwtc/turbsim.html` online; Accessed on 29-07-2021